Chromosomal transposition of *PiggyBac* in mouse embryonic stem cells

Wei Wang*, Chengyi Lin†, Dong Lu*, Zeming Ning*, Tony Cox*, David Melvin*, Xiaozhong Wang†, Allan Bradley*, and Pentao Liu*‡

*The Wellcome Trust Sanger Institute, Wellcome Trust Genome Campus, Hinxton, Cambridgeshire CB10 1SA, United Kingdom; and †Department of Biochemistry, Molecular Biology and Cell Biology, Northwestern University, Evanston, IL 60208

Edited by Kathryn V. Anderson, Sloan–Kettering Institute, New York, NY, and approved April 7, 2008 (received for review February 1, 2008)

Transposon systems are widely used for generating mutations in various model organisms. *PiggyBac* (*PB*) has recently been shown to transpose efficiently in the mouse germ line and other mammalian cell lines. To facilitate *PB*'s application in mammalian genetics, we characterized the properties of the *PB* transposon in mouse embryonic stem (ES) cells. We first measured the transposition efficiencies of *PB* transposon in mouse embryonic stem cells. We next constructed a *PB*/*SB* hybrid transposon to compare *PB* and *Sleeping Beauty* (*SB*) transposon systems and demonstrated that *PB* transposition was inhibited by DNA methylation. The excision and reintegration rates of a single *PB* from two independent genomic loci were measured and its ability to mutate genes with gene trap cassettes was tested. We examined *PB*'s integration site distribution in the mouse genome and found that *PB* transposition exhibited local hopping. The comprehensive information from this study should facilitate further exploration of the potential of *PB* and *SB* DNA transposons in mammalian genetics.

ES cell | *Sleeping Beauty* | transposon

DNA transposons are genetic elements that can relocate between genomic sites by a "cut and paste" mechanism. Since the discovery of the first DNA transposon in maize by Barbara McClintock (1), these elements have been extensively used for genetics and functional genomics in different organisms (2–7).

Sleeping Beauty was the first DNA transposon system shown to be functional in mammalian cells. It has been tested for insertional mutagenesis in the mouse and rat germ lines (8–13), but its relatively low transposition efficiency and strong "local hopping" tendency limit its application in genome-wide screens. However, *SB* has successfully been used to screen for new cancer genes (14, 15).

PiggyBac was isolated from *Trichoplusia ni* (16) and subsequently found to transpose efficiently in many different species (5, 17–19). One important feature of the *PB* transposon is that it nearly always excises itself precisely and leaves no footprint behind (5, 20, 21). It was demonstrated that *PB* was very efficient for germ-line mutagenesis in the mouse (22, 23). It was subsequently confirmed that *PB* has significantly higher transposition activity in mammalian cell lines than *SB* and *Tol2* (24). These studies suggest that *PB* has wide applications in dissecting gene functions (25).

To facilitate *PB*'s application in mammals, we have characterized further the properties of the *PB* transposon. We measured the transposition efficiencies of *PB* in mouse ES cells. We also constructed a *PB*/*SB* hybrid transposon to compare the *PB* and *SB* transposon systems in ES cells. Our data demonstrated that *PB* transposition was inhibited by DNA methylation. We then measured the excision and reintegration rates of a single *PB* transposon from two independent genomic loci and tested its ability to mutate a genomic locus with gene trap cassettes. Finally, we investigated *PB*'s integration site distribution in the mouse genome and found that at least 9% of transposition events from the *Rosa26* locus were local. Our study provides fundamental information on the characteristics of *PB* transposition, enabling the potential of the DNA transposons to be explored for mammalian genetics.

Results

***Efficient PB* Transposition in Mouse ES Cells.** To explore the possibility of using *PB* for mutagenesis in mouse ES cells, we constructed a *PB* transposon that contained a *PGK-Neo-bpA* cassette, which enabled us to score random transposition events by G418 resistance because of the relative position-independent activities of the *PGK* promoter (Fig. 1*A*). The helper plasmid (*CAGG-PBase*) was designed to ubiquitously express *PB* transposase (Fig. 1*A*). Transposition was achieved by coelectroporation of the two plasmids into ES cells. The transposition efficiencies were calculated as the percentage of G418 resistant ($G418^R$) cells over the total cells surviving electroporation.

To determine the optimal condition for transposition, different amounts of the supercoiled *PB-PGK-Neo-bpA* donor and *CAGG-PBase* helper plasmids were used (Fig. 1 *B* and *C*). Using high concentration of both plasmids (50 μg of each), transposition efficiencies approached 28% of cells surviving electroporation. This result indicated that, at high DNA concentrations, essentially all of the cells receiving both the *PB* donor and helper plasmids would have transposition events, based on the assumption that approximately half of cells would receive one plasmid under the electroporation condition used in this study.

We noticed that the transposition efficiency differed with respect to increasing amounts of donor and helper plasmids [Fig. 1 *B* and *C* and supporting information (SI) Fig. S1]. For example, the transposition efficiencies improved 14-fold when the amount of donor DNA being increased from 1 to 50 μg. However, transposition efficiencies were only four times higher when the helper DNA was increased from 1 to 50 μg. Thus, the availability of sufficient transposon DNA was more important to increasing overall transposition rates than levels of *PB* transposase. Nevertheless, at least at the levels tested, there did not appear to be an inhibition of *PB* transposition caused by overdoses of the transposase in the mouse ES cells. This result is in agreement with two recent studies (26, 27) in human and mouse cells, but it contradicts the study in ref. 24.

Using higher concentrations of donor or helper plasmids in the coelectroporation experiments improved the overall transposition efficiencies and increased the transposition events per cell. As shown in Fig. 1*D*, in the experiment with 1 μg of *PB-PGK-Neo-bpA* and 1 μg of *CAGG-PBase*, one to two transposition events were observed in the $G418^R$ colonies. The average copy numbers of *PB* increased to five if 50 μg of each plasmid was used. In some clones, >15 integration sites were visible.

Author contributions: W.W. and P.L. designed research; W.W., C.L., D.L., Z.N., T.C., D.M., X.W., and P.L. performed research; W.W., C.L., and X.W. contributed new reagents/analytic tools; W.W., D.L., Z.N., T.C., D.M., A.B., and P.L. analyzed data; and W.W., A.B., and P.L. wrote the paper.

The authors declare no conflict of interest.

This article is a PNAS Direct Submission.

Freely available online through the PNAS open access option.

‡To whom correspondence should be addressed. E-mail: pl2@sanger.ac.uk.

This article contains supporting information online at www.pnas.org/cgi/content/full/0801017105/DCSupplemental.

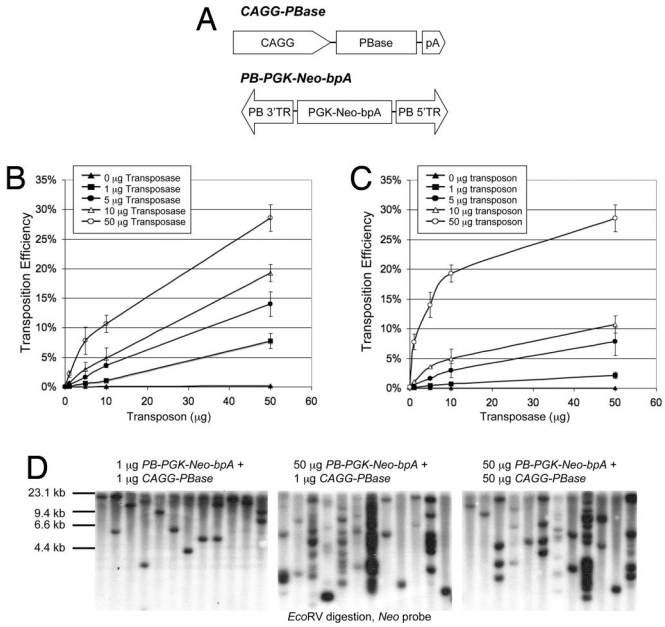

Fig. 1. *PB* transposition in the mouse ES cells. (*A*) Schematic of the *PB* transposase (helper) and transposon (donor) constructs. (*B*) *PB* transposition with increasing amounts of *PB* transposon. A fixed amount of *CAGG-PB*ase was coelectroporated with increasing amounts of *PB-PGK-Neo-bpA* donor plasmid. Each number is the average obtained from three independent experiments. Error bars indicate the standard deviation from the mean. (*C*) *PB* transposition with increasing amounts of *PB* transposase. A fixed amount of *PB-PGK-Neo-bpA* transposon was coelectroporated with increasing amounts of *CAGG-PBase* helper plasmid. (*D*) Southern analysis of *PB* transposition events. Twelve G418^R colonies were picked from each experiment. There is a unique EcoRV site in the *PB-PGK-Neo-bpA* transposon. Genomic DNA was digested with EcoRV and hybridized with a *Neo* probe. Variation of the EcoRV fragment size illustrates independent *PB* transposition events.

***PB-SB* Hybrid Transposon Can Be Mobilized by both Transposases.** To compare the *SB* and *PB* transposon systems, we constructed a hybrid transposon (*PB-SB-PGK-Neo-bpA*) by inserting a *SB-PGK-Neo-bpA* transposon cassette into an intact *PB* transposon (Fig. 2*A*). When coelectroporated with *CAGG-PBase* into ES cells, this new transposon functioned nearly as efficiently as the original *PB-PGK-Neo-bpA* transposon (data not shown).

To compare *PB* and *SB* transposition in an identical genetic background, we constructed two ES cell lines, *Rosa-PBase* and *Rosa-SB11*, by targeting *PB* or *SB* transposase into the *Rosa26* locus in AB2.2 ES cells, respectively (Fig. 2*A*). The transposition efficiencies were measured by transfecting different amounts of *PB-SB-PGK-Neo-bpA* into both cell lines (Fig. 2*B* and Table S1). *PB* transposition efficiency in *Rosa-PB*ase cells was two to three orders of magnitude higher than that of *SB* in *Rosa-SB11* cells (Fig. 2*B*).

To measure the maximum transposition rate in the presence of a constitutive *PB* transposase, we electroporated 50 μg of the *PB-SB-PGK-Neo-bpA* donor plasmid into the *Rosa-PBase* cells. More than half of the cells surviving electroporation became G418^R, demonstrating the extremely efficient *PB* transposition in mouse ES cells (data not shown). In addition to the difference of transposition efficiency, we found that all of the G418^R *Rosa-PBase* clones contained multiple integration sites, whereas most of the G418^R *Rosa-SB11* clones only had single transposon integrations (Fig. 2*C*).

To investigate whether *SB* and *PB* transposases might interfere with each other, we coelectroporated the *PB-SB-PGK-Neo-bpA* and *CAGG-PBase* plasmids into *Rosa-SB11* cells or the wild-type AB2.2 ES cells respectively. No significant difference in transposition rates was noticed from these two electroporations (data not shown), demonstrating that *PB* and *SB* elements in the *PB*/*SB* transposon transposed independently.

***PB* Transposition Is Inhibited by DNA Methylation of the Transposon.** Methylation of the *SB* transposon was reported to increase its transposition efficiency (28–31). To investigate whether methylation had similar effects on the *PB* transposition, we constructed a *PB-SB-SA-βgeo* transposon (Fig. 2*A*). Methylation of the transposon should not affect expressing of *βgeo* because the expression of this gene trapping cassette is determined by endogenous promoters once it is transposed into the genome. The *PB-SB-SA-βgeo* hybrid transposon thus enabled us to compare DNA methylation effects on *PB* and *SB* transposon systems directly, using the same methylated DNA molecules.

PB-SB-SA-βgeo was methylated by a CpG methylase, *M.SssI in vitro*. We transfected an equal amount of methylated and unmethylated *PB-SB-SA-βgeo* DNA into *Rosa-PBase* or *Rosa-SB11* cells, respectively (Fig. 2 *D* and *E* and Table S1). Methylation of the transposon improved the *SB* transposition efficiency by 9-fold (Fig. 2*D*), which is consistent with previous reports. In contrast, *PB* transposition rates were decreased 12-fold by methylation (Fig. 2*E*). This observation was confirmed in mouse fibroblast cells (NIH/3T3) (data not shown), suggesting that inhibition of *PB* transposition by DNA methylation was not specific to mouse ES cells.

Transposition of a Single *PB-SB* Transposon from the *Rosa26* Locus. In the previous experiments, we measured the efficiencies of transposition from plasmids to the chromosomes. To measure the transposition efficiency of a single *PB* transposon at a genomic locus, we constructed a *PGK-[PB-SA-βgeo-PGK-Bsd]-Puro* cassette and targeted it to the *Rosa26* locus, using the *PGK-Bsd* cassette as the selection marker (Fig. 3*A*). This cassette was designed so that excision of the transposon would place a *PGK* promoter immediately in front of the *Puro* coding sequence, allowing the excision events to be scored by puromycin resistance (Puro^R). A bovine growth hormone polyadenylation signal sequence (*bpA*) probe was used to detect three copies of the *bpA* sequence that are present both inside and outside the transposon in the targeted cassette. This probe can be used to detect the excision and the reintegration of the transposon (Fig. S2).

To mobilize the transposon, *CAGG-PB* transposase plasmid was transiently expressed in the *PGK-[PB-SB-SAβgeo-PGK-Bsd]-Puro* knockin cells. Excision events (Puro^R) were detected in 0.70% of cells that survived electroporation (Fig. 3*B*), which were also confirmed by Southern blot analysis (Fig. 3 *A* and *C* and Fig. S2). Of the 246 Puro^R ES cell clones examined, 100 (41%) retained the transposon fragment, suggesting that less than half of the excised transposon had reintegrated into the genome.

***PB* as a Mutagen in ES Cells.** In the last 20 years, gene trapping has been widely used to generate mutations in ES cells (32). To explore the possibility to use *PB* for genome-wide mutagenesis in mouse ES cells, we coelectroporated *PB-SB-SA-βgeo* and *CAGG-PBase* plasmids into AB1 ES cells. From one electroporation (50 μg of each), we typically obtained 50,000–100,000 G418^R colonies, which represented ≈5% of all surviving ES cells.

To estimate the mutagenesis rate, we elected to select for disruption of the mouse *Hprt* gene, which spans ≈40 kb on the X chromosome (Fig. 4*A*). Because AB1 ES cells are male, *PB-SB-SA-βgeo* integration into the *Hprt* locus could result in loss of *Hprt* activity and resistance to 6-thioguanine (6-TG). We transfected AB1 cells with high concentrations of *CAGG-PBase* and *PB-SB-SA-βgeo* plasmids (50 μg of each). The transfected cells were first selected in G418 for the gene trapping events, and subsequently with 6-TG for the loss of *Hprt* function. The mutation rate was calculated as the percentage of 6-TG^R cells vs. all of the trapped (G418^R) cells. We recovered one 6-TG^R colony from every 2,500

GENETICS

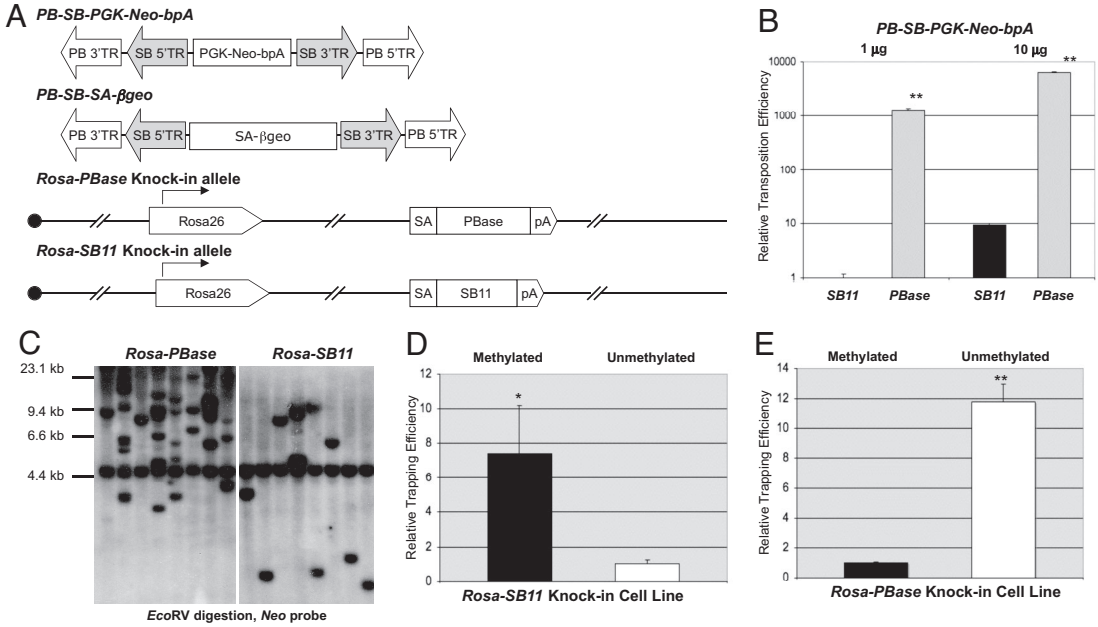

Fig. 2. Direct comparison of *PB* and *SB* transposases, using the *PB/SB* hybrid transposons. (*A*) Schematic of *PB/SB* hybrid transposons, *PBase*, and *SB11* transposase knockin cells lines. (*Upper*) *PB-SB-PGK-Neo-bpA* and *PB-SB-SA-βgeo* hybrid transposons. (*Lower*) Schematic diagram of the *Rosa-PBase* and *Rosa-SB11* alleles. (*B*) Transposition efficiencies of the *PB-SB-PGK-Neo-bpA* hybrid transposon in *Rosa-PBase* and *ROSA-SB11* knockin cell lines. *SB* transposition efficiency (1 μg of *PB-SB-PGK-Neo-bpA*) was arbitrarily used as the standard. There was a 1,310-fold difference between these two lines ($P < 0.002$) when 1 μg of the transposon DNA was used. The fold change dropped to 675-fold ($P < 0.001$) when 10 μg of the *PB-SB-PGK-Neo-bpA* transposon plasmid was used. (*C*) Southern blot analysis of transposition events in *Rosa-PBase* and *Rosa-SB11* knockin lines. Eight G418 resistant colonies were picked from the *PB* or *SB* transposition experiments. Genomic DNA was digested with EcoRV and hybridized against a *Neo* probe. The 5-kb EcoRV fragment present in each clone comes from the insertion of a nonfunctional *Neo* cassette at the *Hprt* locus in AB2.2 cells. Other fragments represented independent transposition events. (*D*) Methylation of the transposon enhanced *SB*-mediated transposition. Methylated and unmethylated *PB-SB-SA-βgeo* DNA was electroporated into *Rosa-SB11* cells. The trapping efficiency was calculated as the percentage of $G418^R$ cells in all of the cells surviving the electroporation. Relative trapping efficiency was normalized to the trapping efficiency of the unmethylated transposon; $P < 0.02$. (*E*) Methylation of the transposon inhibited *PB*-mediated transposition. The same experiment was performed in *Rosa-PBase* cells as in *D*; $P < 0.002$.

$G418^R$ clones, representing a mutation rate of 0.04% under this condition.

Splinkerette PCR amplification of the flanking genomic fragments identified the transposon integration sites in introns 1, 2, and 4 of *Hprt* gene in five independent 6-TG^R resistant clones (Fig. 4*B*). *Hprt-LacZ* fusion transcripts were identified in three independent clones by RT-PCR (Fig. S3), confirming that the resistance to 6-TG in these clones was caused by *PB* integration. In another 6-TG^R clone, *PB* had integrated in the opposite orientation. RT-PCR identified a fusion transcript in which an insertion of a 74-bp sequence from *PB 5′TR* caused a frame shift in the *Hprt* coding sequence (Fig. S4). This result suggests that the *PB 5′TR* contains a pair of cryptic splice acceptor and donor sequences.

To determine the efficiency of remobilization from the *Hprt* locus, we expressed *PB* transposase in four independent 6-TG^R cell lines, including the clone trapped by the *PB 5′TR* (Fig. 4*A*). Excision of the transposon restored the function of *Hprt* and HAT^R clones were recovered from all four cell lines transfected with *PB* transposase. An average excision rate of 0.86% was observed at the *Hprt* locus (Fig. 3*B*), which is comparable with that at the *Rosa26* locus.

Because the *PB/SB* hybrid transposon integrated into the introns of *Hprt* gene, we tested mobilization *by* SB transposase (*CMV-SB11*) in two of the four 6-TG^R lines. The excision rate was $\approx 10^{-5}$ (data not shown), similar to that reported for the *Hprt* locus (33). Therefore, the *PB-SB* hybrid transposon could be remobilized by the second transposase (*SB*) after the initial *PB* transposition. Interestingly, expression of *SB* transposase in the clone trapped by *PB 5′TR* did not generate HAT^R colonies, suggesting that the residual *PB* repeats could still disrupt the *Hprt* locus owing to the cryptic splicing donor and acceptor sequences in the *PB 5′TR*.

Precise Excision of PB. *PB* transposition has been shown to be nearly precise in fruitfly (5, 20, 21). To confirm this observation, we examined *PB* excision footprints from 32 independent excision events from the *Rosa26* locus and 30 from the *Hprt* locus. Sequence analysis of the junction fragments between *PGK* promoter and *Puro* coding sequence or the *Hprt* genomic fragments flanking the original *PB* integration site showed all but three had a precise excision (Fig. 4*C*). Thus, 95% of the genomic *PB* transposon excision events (*Rosa26* and *Hprt*) were precise in ES cells.

Distribution of PB Integration Sites in the Genome and PB Local Hopping. To obtain a comprehensive view of the distribution of the *PB* in the mouse genome, we cloned the insertion junctions and mapped these back to the genome.

A total of 945 unique integration sites were characterized from $G418^R$ clones generated by coelectroporation of high concentrations (50 μg of each) of the *CAGG-PBase* and *PB-SB-PGK-Neo-bpA* plasmids (Fig. 5*A* and Dataset S1). Analysis of these random integration sites revealed that they were distributed evenly across the genome (Dataset S2). Approximately 43% of these integration sites are located in Ensembl (version 48.37a) annotated genes, which is in agreement with other observations that *PB* has a tendency to integrate into transcription units (22, 26).

467 *PB* integration sites from the gene trapping of *PB-SB-SA-βgeo* plasmids were also identified (Fig. 5*B* and Dataset S3 and Dataset S4). These sites were compared with the Ensembl GeneTrap database and at least 26 genes trapped by *PB* were not currently trapped by the existing vectors (Dataset S5), confirming that *PB* transposition indeed provided an efficient alternative mutagen for mouse genetics.

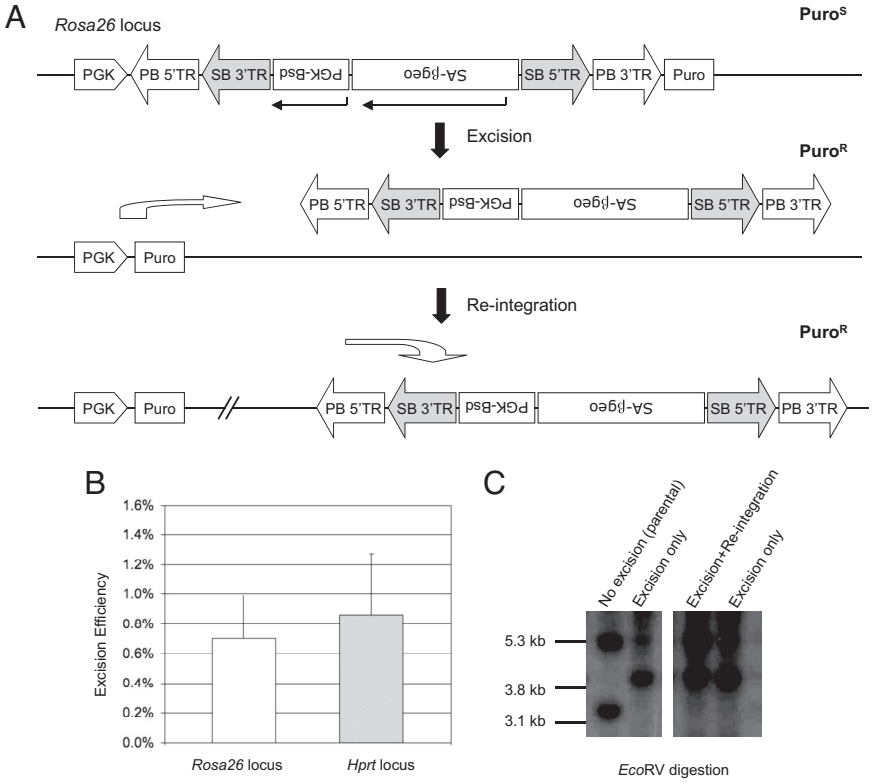

Fig. 3. Re-mobilization of *PB/SB* hybrid transposon. (*A*) Illustration of the *PGK-[PB-SB-SA-βgeo-PGK-Bsd]-Puro* knockin allele at the *Rosa26* locus. A *SA-βgeo* trapping cassette and a *PGK-Bsd* selection cassette were cloned into the *PB/SB* hybrid transposon to form the *PB-SB-SA-βgeo-PGK-Bsd* transposon. This complex transposon was subsequently inserted in between the *PGK* promoter and the *Puro* coding sequence in a *PGK-Puro* cassette and targeted to the *Rosa26* locus. Transfection of the targeted ES cells with *CAGG-PBase* plasmid mobilized the targeted transposon. Excision reunited the *PGK* promoter and *Puro* coding sequence so that the excision events can be scored by puromycin resistance. (*B*) Transposon excision rates from the *Rosa26* and *Hprt* loci. *CAGG-PBase* DNA were electroporated into *Rosa-PGK-[PB-SB-SA-βgeo-PGK-Bsd]-Puro* targeted cells to mobilize the transposon. The excision rate was adjusted to account for all of the cells surviving the electroporation. Similar experiments were carried out in the cells that the *PB-SB-SA-βgeo* transposon inserted into the *Hprt* locus (see Fig. 4). (*C*) Southern blot analysis of the excision events from the *PGK-[PB-SB-SAβgeo-PGK-Bsd]-Puro* knockin cells. The original targeted clone had both the 3.1-kb targeted EcoRV band and the 5.3-kb transposon fragment. Clones that lost *PB* after excision only have the 3.8-kb excision fragment. Clones in which transposon excision was followed by reintegration had both the 3.8-kb excision and 5.3-kb transposon fragments.

Excision of a single copy of transposon from either *Rosa26* or *Hprt* provided an opportunity to examine with a large dataset whether *PB* transposition exhibited any evidence of local hopping. Of 264 new insertions excised from the *Rosa26* locus (Fig. 5*C*, Dataset S6, and Dataset S7), 18% of these sites were on the donor chromosome (chromosome 6). Interestingly, 47% of the new integration sites on chromosome 6 (21/47), or 9% (21/264) of the total reintegration sites, were clustered within a 100-kb region flanking the *Rosa26* locus, with the rest of the integration sites being relatively evenly distributed across the genome. It was apparent from these data that *PB* transposition still had some degrees of local hopping but much less severe than *SB* transposition.

To investigate the local hopping property of *PB* transposition at another locus, we cloned 93 new integration sites from *PB* transposition from the *Hprt* locus. However, analysis of these sites did not reveal any obvious bias to either the *Hprt* locus or the X chromosome (Fig. 5*D* and Dataset S8). This can be explained by the possibility that local reintegration sites were still

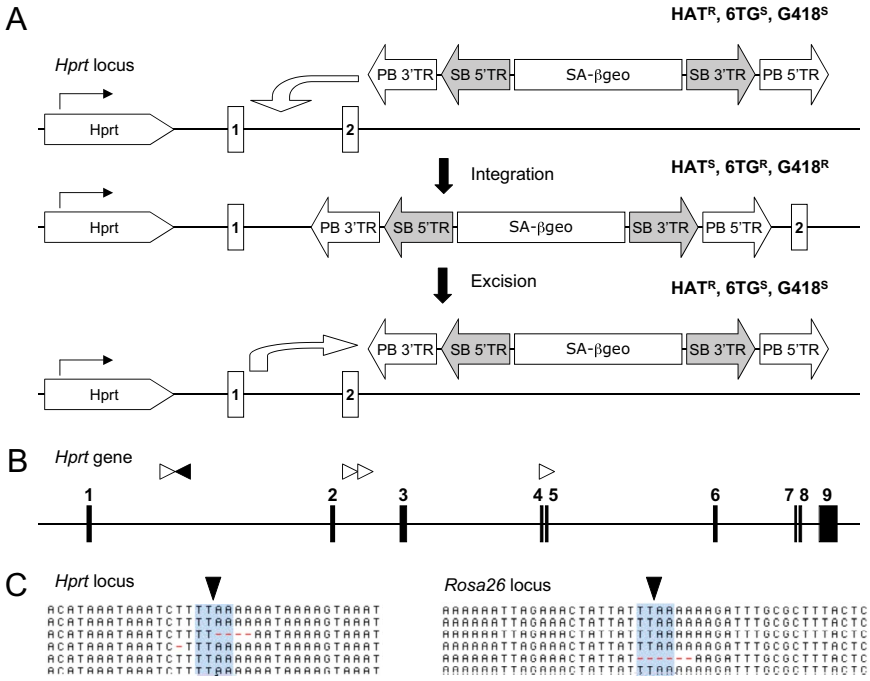

Fig. 4. *PB*-mediated mutagenesis. (*A*) Schematic illustration of a *PB-SB-SA-βgeo* transposon integrated into the *Hprt* locus. AB1 ES cells have one copy of *Hprt* gene. If a *PB-SB-SA-βgeo* transposon integrates into *Hprt* locus and disrupts its function, AB1 ES cells will become HAT sensitive and 6-TG resistant. If this transposon is remobilized, the cells will become HAT resistant and 6-TG sensitive. (*B*) Transposon insertions in the *Hprt* locus. Transposon-genomic junction fragments from five 6-TG clones were mapped to the *Hprt* locus. Filled boxes, *Hprt* exons; white arrowhead, transposon integration sites of clones in which the *Hprt* exons were directly spliced the *SA-βgeo* cassette; black arrowhead, the transposon integration site of a clone in which the *Hprt* gene was disrupted by *PB 5′TR*. (*C*) Nearly precise excision of the *PB* transposon from the *Hprt* and *Rosa26* loci. PCR products that amplify the excision sites in 30 independent excision events from the *Hprt* locus and 32 from the *Rosa26* locus were sequenced. All but three excision events were precise. One clone had a 4-bp microdeletion, another had a 1-bp deletion, and the third had a 6-bp microdeletion.

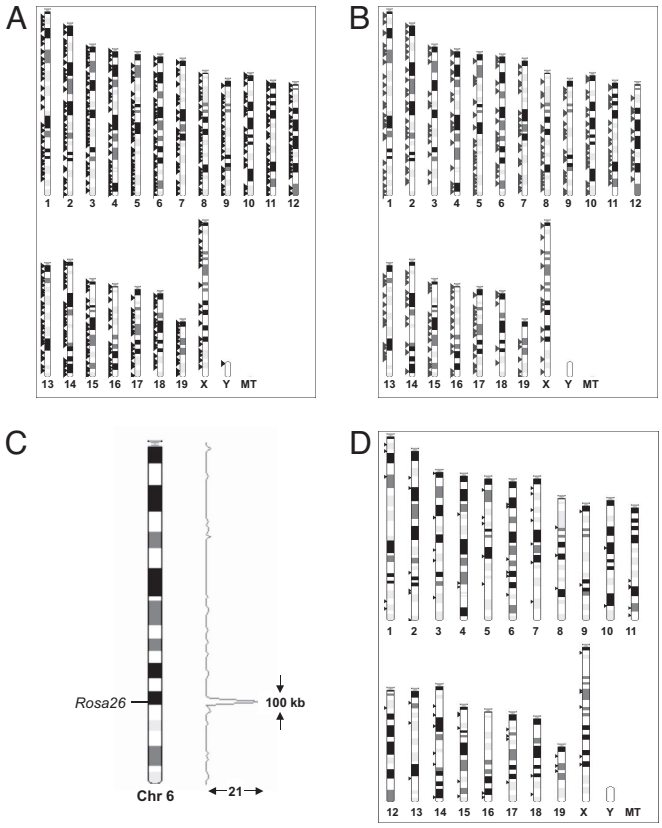

Fig. 5. Distribution of *PB* integration sites in the genome. (*A*) *PB* integration sites in the mouse genome from random transposition events. The sites were identified from transposition experiments, using *CAGG-PBase* and *PB-SB-PGK-Neo-bpA*. The transposon-genomic junction fragments were mapped to the mouse genome and displayed in Ensembl (version 48.37a). (*B*) *PB* integration sites of gene trapping clones. Splinkerette PCR was performed on $G418^R$ clones from coelectroporation of *CAGG-PBase* and *PB-SB-SA-βgeo*. Transposon-genomic junction fragments were then mapped to the mouse genome. (*C*) Local hopping of *PB* transposition from the *Rosa26* locus. Nine percent of *PB* reintegration sites (21/264) were clustered within a 100-kb region flanking the *Rosa26* locus on the donor chromosome (chr. 6). The rest of the integration sites appeared to be randomly distributed in the genome. The height of the peaks on the histograph represent the number of integration sites in a genomic region. (*D*) No apparent local hopping of the *PB* transposition from the *Hprt* locus. A total of 93 integration sites were cloned from *PB* transposition from the *Hprt* locus. Analysis of these sites did not show any obvious bias to either the *Hprt* locus or the X chromosome.

inside the *Hprt* locus because of the narrow "local hopping" window. Therefore, these reintegration events still disrupted the *Hprt* locus and could not be scored by HAT selection. Alternatively, the limited local hopping of *PB* transposition may be specific to certain genomic loci. It is also possible that during HAT selection there was more time for remobilization compared with Puro selection.

Discussion

In this report, we analyzed the basic properties of *PB* transposition in mouse embryonic stem cells. The extremely efficient vector-chromosome transposition make *PB* an excellent vehicle to efficiently deliver genetic elements into mammalian cells. Our data also argued against the existence of transposase overproduction inhibition in ES cells at the conditions tested. This unique property of *PB* provides a convenient avenue for further improving *PB* transposition in mammalian cells.

Local hopping is a property of most DNA transposons. In mouse ES cells, the frequency of local transposition of *PB* transposon system is much lower than that of *SB* (50%) (33). The local hopping interval of *PB* (≈100 kb) is smaller than that of *SB* (≈5 Mb) (13, 34). The local transposition feature of *PB* has not been reported either in *Drosophila melanogaster* (5, 35) or in the mouse (22). One explanation is that we transiently expressed *PBase* in ES cells, whereas the transposase in the transgenic *Drosophila* or mouse lines was constitutively expressed (22) or continuously induced (35) in the germ line. This explanation is supported by the elimination of local hopping in embryos and in tumors when *SB* transposase is constitutively expressed (15). It is possible that the lack of local hopping in *PB* transposition observed in previous studies was due to multiple rounds of *PB* transposition.

Interestingly, only 40% of the *PB* excision events were accompanied with reintegration of the transposon, compared with the 77% reintegration rate reported for *SB* in a similar setting (33). It is likely that this relatively low reintegration rate is also due to multiple rounds of excision/reintegration. Frequent transposition can help to reduce local hopping, but it also increases the possibility of leaving footprint mutations and generating chromosomal rearrangements (36). To minimize these potential side effects, tissue-specific or drug-inducible (27) *PB* transposase lines might be necessary for somatic and germ-line mutagenesis in the mouse.

Our study, together with those from other groups (22, 24, 26), indicate that *PB* transposition is more efficient than *SB* or other DNA transposons in mammalian cells. However, *PB* and *SB* have distinct biological properties that can be used separately or together. The *PB*/*SB* hybrid transposon, combining the unique properties of *PB* and *SB*, provides a complementary transposon tool kit for mouse geneticists, just like *PB* and *P* element in *D. melanogaster* (5). One possible application of the *PB*/*SB* hybrid transposon is to use *PB* as a vehicle to transpose to a genomic region of interest, and subsequently to employ *SB* to achieve regional saturation mutagenesis (13), taking advantage of *SB*'s strong local hopping.

In summary, we have demonstrated here that the *PB* transposition is highly efficient in mouse ES cells, has local hopping tendency. In contrast to *SB*, *PB* transposition is inhibited by DNA methylation. *PB* transposons carrying gene-trapping cassettes served as excellent mutagens and can be potentially used in the large-scale mouse mutagenesis programs. Detailed analysis of *PB* integration sites indicated that most mouse genomic regions are accessible to *PB* transposition. Finally, the unique characteristics of the *PB* transposon make it possible to combine it with other existing mutagens, especially *SB*, to provide a broader and less biased coverage of the mouse genome.

Materials and Methods

Plasmid Construction and Cell Transfection. See *SI Material and Methods*.

Splinkerette PCR. *PB* integration sites were determined by splinkerette PCR (37). Drug resistant colonies were pooled together, and genomic DNA was extracted from ES cells using standard protocols. *Sau*3AI digested genomic DNA was ligated with splinkerette and junction fragments were PCR amplified with primers HMSp1 (5′-CGA AGA GTA ACC GTT GCT AGG AGA GAC C-3′) and *PB*-R-Sp1 (5′-CCT CGA TAT ACA GAC CGA TAA AAC ACA TGC-3′). Nested PCR was performed by using primers HMSp2 (5′-GTG GCT GAA TGA GAC TGG TGT CGA C-3′) and *PB*-R-Sp2 (5′-ACG CAT GAT TAT CTT TAA CGT ACG TCA CAA-3′). PCR products were cloned into pZero2.0-TOPO (Invitrogen) and shot-gun sequenced by using M13 forward and reverse primers.

Southern Analysis. For *PB-SB-PGK-Neo-bpA* and *PB-SB-SA-βgeo* transposition, we have used a *Neo* probe to detect *PB* or *SB* mediated transposition. There is a unique *Eco*RV site in both transposons. Variation in the sizes of the *Eco*RV fragments indicated different *PB* transposition events.

For *PGK-[PB-SB-SAβgeo-PGK-Bsd]-Puro* single transposon remobilization, we used a *bpA* probe to detect excision and reintegration at *Rosa26* locus. *Eco*RV digestion will identify two restriction fragments, 3.1 kb and 5.3 kb, in transposon targeted clones. When the transposon is mobilized, the 3.1-kb fragment changes to 3.8 kb. The 5.3-kb *Eco*RV fragment will remain if excised transposon reintegrates into the ES cell genome.

ACKNOWLEDGMENTS. We thank Roland Rad, Juan Cadinanos, Qi Liang, Song Choon Lee, Qin Su, and Mariaestela Ortiz for critical reading of the manuscript and Nancy Holroyd, Jim Stalker, and Stephen Rice for excellent technical assistance. This work was funded by the Wellcome Trust (A.B. and P.L.), National Institutes of Health Grant 5R21GM079528 (to X.W.), and the Illinois Department of Public Health (X.W.).

1. McClintock B (1950) The origin and behavior of mutable loci in maize. *Proc Natl Acad Sci USA* 36:344–355.
2. Hayes F (2003) Transposon-based strategies for microbial functional genomics and proteomics. *Annu Rev Genet* 37:3–29.
3. Spradling AC, Rubin GM (1982) Transposition of cloned P elements into Drosophila germ line chromosomes. *Science* 218:341–347.
4. Bellen HJ, *et al.* (1989) P-element-mediated enhancer detection: A versatile method to study development in Drosophila. *Genes Dev* 3:1288–1300.
5. Thibault ST, *et al.* (2004) A complementary transposon tool kit for Drosophila melanogaster using P and piggyBac. *Nat Genet* 36:283–287.
6. Plasterk RH (1996) The Tc1/mariner transposon family. *Curr Top Microbiol Immunol* 204:125–143.
7. Osborne BI, Baker B (1995) Movers and shakers: Maize transposons as tools for analyzing other plant genomes. *Curr Opin Cell Biol* 7:406–413.
8. Dupuy AJ, Fritz S, Largaespada DA (2001) Transposition and gene disruption in the male germline of the mouse. *Genesis* 30:82–88.
9. Fischer SE, Wienholds E, Plasterk RH (2001) Regulated transposition of a fish transposon in the mouse germ line. *Proc Natl Acad Sci USA* 98:6759–6764.
10. Horie K, *et al.* (2001) Efficient chromosomal transposition of a Tc1/mariner-like transposon Sleeping Beauty in mice. *Proc Natl Acad Sci USA* 98:9191–9196.
11. Horie K, *et al.* (2003) Characterization of Sleeping Beauty transposition and its application to genetic screening in mice. *Mol Cell Biol* 23:9189–9207.
12. Kitada K, *et al.* (2007) Transposon-tagged mutagenesis in the rat. *Nat Methods* 4:131–133.
13. Keng VW, *et al.* (2005) Region-specific saturation germline mutagenesis in mice using the Sleeping Beauty transposon system. *Nat Methods* 2:763–769.
14. Collier LS, *et al.* (2005) Cancer gene discovery in solid tumours using transposon-based somatic mutagenesis in the mouse. *Nature* 436:272–276.
15. Dupuy AJ, *et al.* (2005) Mammalian mutagenesis using a highly mobile somatic Sleeping Beauty transposon system. *Nature* 436:221–226.
16. Cary LC, *et al.* (1989) Transposon mutagenesis of baculoviruses: Analysis of Trichoplusia ni transposon IFP2 insertions within the FP-locus of nuclear polyhedrosis viruses. *Virology* 172:156–169.
17. Lobo N, Li X, Fraser MJ, Jr (1999) Transposition of the piggyBac element in embryos of Drosophila melanogaster, Aedes aegypti and Trichoplusia ni. *Mol Gen Genet* 261:803–810.
18. Handler AM, Harrell RA, 2nd (1999) Germline transformation of Drosophila melanogaster with the piggyBac transposon vector. *Insect Mol Biol* 8:449–457.
19. Bonin CP, Mann RS (2004) A piggyBac transposon gene trap for the analysis of gene expression and function in Drosophila. *Genetics* 167:1801–1811.
20. Fraser MJ, Ciszczon T, Elick T, Bauser C (1996) Precise excision of TTAA-specific lepidopteran transposons piggyBac (IFP2) and tagalong (TFP3) from the baculovirus genome in cell lines from two species of Lepidoptera. *Insect Mol Biol* 5:141–151.
21. Elick TA, Bauser CA, Fraser MJ (1996) Excision of the piggyBac transposable element in vitro is a precise event that is enhanced by the expression of its encoded transposase. *Genetica* 98:33–41.
22. Ding S, *et al.* (2005) Efficient transposition of the piggyBac (PB) transposon in mammalian cells and mice. *Cell* 122:473–483.
23. Wu S, Ying G, Wu Q, Capecchi MR (2007) Toward simpler and faster genome-wide mutagenesis in mice. *Nat Genet* 39:922–930.
24. Wu SC, *et al.* (2006) piggyBac is a flexible and highly active transposon as compared to sleeping beauty, Tol2, and Mos1 in mammalian cells. *Proc Natl Acad Sci USA* 103:15008–15013.
25. Feschotte C (2006) The piggyBac transposon holds promise for human gene therapy. *Proc Natl Acad Sci USA* 103:14981–14982.
26. Wilson MH, Coates CJ, George AL, Jr (2007) PiggyBac Transposon-mediated Gene Transfer in Human Cells. *Mol Ther* 15:139–145.
27. Cadinanos J, Bradley (2007) A Generation of an inducible and optimized piggyBac transposon system. *Nucleic Acids Res* 35:e87.
28. Ikeda R, *et al.* (2007) Sleeping beauty transposase has an affinity for heterochromatin conformation. *Mol Cell Biol* 27:1665–1676.
29. Park CW, Kren BT, Largaespada DA, Steer CJ (2005) DNA methylation of Sleeping Beauty with transposition into the mouse genome. *Genes Cells* 10:763–776.
30. Park CW, Park J, Kren BT, Steer CJ (2006) Sleeping Beauty transposition in the mouse genome is associated with changes in DNA methylation at the site of insertion. *Genomics* 88:204–213.
31. Yusa K, Takeda J, Horie K (2004) Enhancement of Sleeping Beauty transposition by CpG methylation: Possible role of heterochromatin formation. *Mol Cell Biol* 24:4004–4018.
32. Skarnes WC, *et al.* (2004) A public gene trap resource for mouse functional genomics. *Nat Genet* 36:543–544.
33. Luo G, Ivics Z, Izsvak Z, Bradley A (1998) Chromosomal transposition of a Tc1/mariner-like element in mouse embryonic stem cells. *Proc Natl Acad Sci USA* 95:10769–10773.
34. Carlson CM, *et al.* (2003) Transposon mutagenesis of the mouse germline. *Genetics* 165:243–256.
35. Hacker U, *et al.* (2003) piggyBac-based insertional mutagenesis in the presence of stably integrated P elements in Drosophila. *Proc Natl Acad Sci USA* 100:7720–7725.
36. Geurts AM, *et al.* (2006) Gene mutations and genomic rearrangements in the mouse as a result of transposon mobilization from chromosomal concatemers. *PLoS Genet* 2:e156.
37. Mikkers H, *et al.* (2002) High-throughput retroviral tagging to identify components of specific signaling pathways in cancer. *Nat Genet* 32:153–159.